Title

T1rho MR properties of human patellar cartilage: correlation with indentation stiffness and biochemical contents

Journal

Skeletal Radiology, 53(4)

ISSN

0364-2348

Authors

Bae, Won C

Statum, Sheronda

Masuda, Koichi

et al.

Publication Date

2024-04-01

DOI

10.1007/s00256-023-04458-6

T1rho MR Properties of Human Patellar Cartilage:

Correlation with Indentation Stiffness and Biochemical Contents

[1,3]Won C. Bae, Ph.D., Associate Professor
[1,3]Sheronda Statum, M.S., M.B.A., Staff Research Associate
[2]Koichi Masuda, M.D., Professor
[1,3]Christine B. Chung, M.D., Professor

[1]Department of Radiology
University of California-San Diego
9427 Health Sciences Drive
La Jolla, CA 92093-0997

[2]Department of Orthopaedic Surgery
University of California-San Diego
9500 Gilman Dr.
La Jolla, CA 92093-0863

[3]VA San Diego Healthcare System
3350 La Jolla Village Drive MC-114
San Diego, CA 92161

Corresponding Author & Sponsoring Institution:
Won C. Bae, Ph.D.
[1]9427 Health Sciences Drive
La Jolla, CA 92093-0997
TEL: (858) 246-2240
FAX: (619) 471-0503
email: wbae@health.ucsd.edu

Submitted to: Skel Rad

Manuscript Type: Scientific Article

T1rho MR Properties of Human Patellar Cartilage:

Correlation with Indentation Stiffness and Biochemical Contents

ABSTRACT

Objective: Cartilage degeneration involves structural, compositional and biomechanical alterations that may be detected non-invasively using quantitative MRI. The goal of this study was to determine if topographical variation in T1rho values correlate with indentation stiffness and biochemical contents of human patellar cartilage.

Design: Cadaveric patellae from unilateral knees of 5 donors with moderate degeneration were imaged at 3-Telsa with spiral chopped magnetization preparation T1rho sequence. Indentation testing was performed, followed by biochemical analyses to determine water and sulfated glycosaminoglycan contents. T1rho values were compared to indentation stiffness, using semi-circular regions of interest (ROIs) of varying sizes at each indentation site. ROIs matching the resected tissues were analyzed, and univariate as well as multivariate regression analyses were performed to compare T1rho values to biochemical contents.

Results: Grossly, superficial degenerative change of the cartilage (i.e., roughened texture and erosion) corresponded with regions of high T1rho values. High T1rho values correlated with low indentation stiffness, and the strength of correlation varied slightly with the ROI size. Spatial variations in T1rho values correlated positively with that of the water content (R^2=0.10, $p<0.05$) and negatively with the variations in

the GAG content (R^2=0.13, p<0.01). Multivariate correlation (R^2=0.23, p<0.01) was stronger than either of the univariate correlations.

Conclusion: These results demonstrate the sensitivity of T1rho values to spatially-varying function and composition of cartilage, and that the strength of correlation depends on the method of data analysis and consideration of multiple variables.

Key Words: Osteoarthritis, knee, glycosaminoglycan, water, biomechanics

INTRODUCTION

Articular cartilage is a thin layer of connective tissue covering the ends of long bones, facilitating joint motion. It is composed of sparsely distributed chondrocytes within a fluid-filled extracellular matrix that consists mainly of collagen and proteoglycans. The latter, due to a high density of negatively charged groups, swell in physiologic solutions and provide resistance to compression [1, 2].

With advancing age in adults, human articular cartilage undergoes degeneration that may advance to osteoarthritis (OA), a joint disease that affects over 60 million Americans [3] and has a large economic impact [4]. OA is a multifactorial disease that can affect multiple components of the knee, including cartilage, meniscus, ligaments, and the bone. Radiographic characteristics of OA include roughening of the articular surface and cartilage loss, meniscal and ligamentous instability due to degeneration and/or tear, and bony changes such as osteophyte formation, subchondral bone sclerosis. Additionally, OA can result in joint pain, limitation of motion, as well as new bone and cartilage formation [5]. Early diagnosis of cartilage degeneration, and the ability to track its progression, would be useful for treatment strategies.

Degenerate and osteoarthritic cartilage exhibits alterations in biochemical content as well as biomechanical weakening. There is a depletion of glycosaminoglycan (GAG) content as well as increased water content near the surface [1, 6], while collagen content may not be affected in early stages [7]. However, collagen network integrity, assessed grossly and biochemically [8], is reduced. These changes are in concert with

biomechanical weakening, as seen in indentation [9-11] and tensile [10, 12] testing of aged or degenerated cartilage. Indentation testing is a non-destructive method of evaluating biomechanical properties of cartilage, and it involves compression of cartilage surface using a small probe to measure mechanical response. Past studies have reported strong correlation between indentation stiffness and glycosaminoglycan content [13] and between tensile stiffness and collagen content near the superficial layer of cartilage [12]. In addition, indentation testing allows for evaluation of local properties of the tissue, which is useful for comparison against local MR properties.

Conventional morphologic MRI has been useful in evaluating the structure of cartilage[14] but not composition or function. GAG-sensitive MRI such as T1rho [15] and delayed gadolinium-enhanced MRI of cartilage (dGEMRIC) [16] have been introduced, with the former not requiring the use of contrast agent. T1rho relaxation time measurement is a promising technique since it does not involve invasive contrast agent injection and waiting duration as needed with dGEMRIC. T1rho techniques are increasingly used to evaluate musculoskeletal tissues as well.

Establishing a relationship between T1rho properties, indentation stiffness [17] and biochemical content of human cartilage would extend the implications of T1rho imaging. The objective of this study was to determine topographic variations in indentation stiffness, water and GAG contents, and T1rho values in human patellar cartilage, and the relationship between the measures.

MATERIALS AND METHODS

Tissue Preparation

This cadaveric study was exempt from institutional review board. Axial bone-cartilage slabs (**Figure 1**), 5 mm thickness, were obtained from the center of patellae of five cadaveric knees (80±4 yrs; grade 3 by Collins grading [18]) and kept hydrated with saline containing proteinase inhibitors [19] to hinder enzymatic degradation. Moderately degenerated samples were chosen to evaluate spatial variations in cartilage degeneration. This ensured that each sample was sourced from different donors. The remaining patellar tissues were used for another unrelated study.

MR Image Acquisition

General Electric 3T Signa HDx was used with a 1" birdcage coil. Each sample was placed into a 1" diameter syringe filled with Fomblin and placed into the coil, whose long axis was in-line with the main magnetic field. A 2-D spiral sequence with T1rho preparation pulse, 2D Spiral Chopped Magnetization Preparation (2D SCMP) [20, 21], was used to obtain 6 images (4 images shown on **Figure 2A to D**) with T1rho-weighting: repetition time (TR) =1500 ms, spin lock time (TSL)=0, 10, 20, 40, 60 and 80 ms, spin lock frequency=500 Hz, number of spirals=85, number of sampling=1024 points, image matrix=256x256, FOV=5 cm, slice=2.4 mm, flip angle=90°.

We determine signal-to-noise ratio (SNR) on T1rho-weighted images acquired at TSL of 80 ms (with the lowest cartilage signal intensity) by dividing the mean signal

intensity of articular cartilage by the standard deviation of the background noise. For the five samples, the mean and standard deviation of the SNR was 95.4 and 8.4, respectively, suggesting a high fidelity.

Biomechanical Testing

Rapid indentation testing [17, 22] was used. Patellar slabs were clamped vertically onto a stage, and sites (~1 mm apart; **Figure 3A**) along the articular surface were tested by a bench top indentation apparatus (V500cs, Biomomentum Inc., Quebec, Canada), fitted with a 0.8 mm diameter plane-ended tip. The stage movement was computer-controlled with 0.01 mm resolution, which allowed for a precise positioning of indentation sites. The sites were aligned perpendicular to the tip, a tare load (3 mN) was applied, followed by 100 μm compression, a hold for 1 s, and a release. Indentation stiffness (where a higher value indicates a stiffer sample) was determined as the resultant force divided by the applied displacement and converted to the units of N/mm [23]. A total of 211 sites were tested on 5 samples (35, 38, 57, 34, and 47 sites for each sample).

Biochemical Contents

Rectangular cartilage fragments (**Figure 4D**, dashed lines), approximately 5 mm wide by 2-3 mm thickness thick, were obtained by resection. Close up photographs were taken with resection of each piece to keep a determine the location of each piece. The fragments were weighed wet and dry, to determine water content. Sulfated GAG

(sGAG) content was determined by dimethyl methylene blue assay,[24] and divided by the wet weight to determine the concentration.

Image Analysis

Region of Interest Selection for Comparison to Indentation Stiffness. Since indentation testing induces a local tissue deformation around the contact area [25], semi-circular ROI (**Figure 3B**) of varying diameters were selected using a semi-automated Matlab (R2009a with Image Processing Toolbox, Mathworks, Natick, MA) routine to ensure correct spacing. Photographs taken during indentation were spatially-registered with MR images to determine contact sites. A single voxel was marked to represent the intersection between articular surface and the central long axis of the indenter. Regions of articular cartilage within 0.6, 1.2, or 2.4 mm radius (or 1.2, 2.4 or 4.8 mm diameter) of the voxel location were included in the semi-circular ROI.

Region of Interest Selection for Comparison to Biochemical Content. Photographs were taken during resection of biochemistry samples and used to create similar ROIs (~rectangular divisions, similar to dashed lines in **Figure 3A**) onto MR images, and to determine average T1rho value within each ROI (**Figure 4E**).

T1rho Quantification. Using Matlab, T1rho maps were first created by voxel-wise mono-exponential fitting (**Figure 2D**) of signal intensity to:

$$SI(TSL) = S_0 \cdot \exp(-TSL/T1rho)$$

where TSL is the spin lock time (6 TSLs), SI(TSL) is the voxel's signal intensity at a given spin lock time, and S_0 and T1rho are the fitted parameters.

For each ROI (i.e., indentation or biochemistry), T1rho values of all voxels were averaged to determine the mean and standard deviation values.

Statistics

To compare biomechanical and MR properties, T1rho values in semi-circular ROIs were compared to indentation stiffness (log-transformed due to a large range) using linear regression (Systat 10, Systat Software Inc., San Jose, CA). Correlation coefficients between indentation stiffness and T1rho values from different-sized ROIs were compared using Fisher r-to-z transformation.

To compare spatial variation in biochemical content with that in MR properties, T1rho values in rectangular ROI were averaged and normalized to the average value of each sample. Normalized T1rho values in rectangular ROI were compared to normalized water and sGAG contents using univariate and multivariate linear regression analyses.

RESULTS

Patellar samples exhibited local areas of cartilage lesions (**Figure 4D, arrows**), which generally corresponded to regions with high T1rho values on the maps (**Figure 4A, arrows**). T1rho maps also exhibited depth-dependent variations (**Figure 4A**). The deeper layers of cartilage had fairly low T1rho values (approximately 50 ms) that increased to approximately greater than 200 ms near the articular surface.

Indentation stiffness correlated significantly with T1rho values near the articular surface. On a given sample, sites with high T1rho values (**Figure 4B**) usually had low indentation stiffness (**Figure 4C**). The strength of correlation between T1rho and indentation stiffness was the highest (R^2=0.25, p<0.0001, **Figure 5B**) when ROI diameter was 2.4 mm, and it was the lowest (R^2=0.22) when ROI diameter was 4.8 mm (**Figure 5C**). However, there were no significant differences between these three correlation coefficients.

There was also significant correlation between spatial distribution of T1rho values and biochemical contents. In general, regions of cartilage with high water content or low GAG content had high T1rho values (**Figure 4EFG**), although this trend may be confounded somewhat by the depth-variations in the GAG content. Spatial variations in T1rho values correlated positively with water content (**Figure 6A**; R^2=0.10, p<0.05) and negatively with GAG content (**Figure 6B**; R^2=0.13, p<0.01). Multivariate correlation (**Figure 6C**; R^2=0.23, p<0.01) was stronger than either of the univariate correlations, suggesting independent contribution of water and GAG content to T1rho values.

DISCUSSION

The results of the study suggested that T1rho properties correlated significantly with biomechanical properties and biochemical contents of human articular cartilage. The inverse relation between T1rho values and indentation stiffness or GAG content, is

consistent with past studies. In a study by Wheaton et al. [26], a negative relation between T1rho values and compressive aggregate modulus was found in experimentally-degenerated bovine cartilage. Additionally, high T1rho values correlated with low GAG content in cartilage [15, 26]. In osteoarthritic cartilage, increased T1rho value are seen in vivo [27, 28], which is consistent with the loss of biomechanical integrity [23, 29] as well as GAG content [29].

The present study extends past studies that evaluated relationship between quantitative MR properties of cartilage and indentation stiffness. Samosky et al. [30] performed indentation testing and dGEMRIC of human tibial plateau cartilage and found that spatial distribution of the values correlated significantly. In the past study, the MR property was determined in a uniform rectangular ROI directly under each indentation site. In our study, semi-circular ROIs were used, in order to better match with the regions of tissue that undergo the highest deformation during indentation testing [25]. Additionally, the consideration of different size of ROI is important for optimizing quantitative analysis of MR data for mechanical properties of cartilage. While only 3 different sizes were considered, we found that the strength of correlation varied slightly with the ROI size, suggesting that an optimal size (and possibly shape) of ROI may exist. These relations can further be verified in vivo, since indentation testing can also be performed in vivo [31, 32], along with MRI.

The result of the multivariate analysis is useful for better understanding of contribution of independent constituents of articular cartilage to T1rho values. While an increase in water content and a decrease in GAG content generally occur together in

osteoarthritis [29] or enzymatic degradation [33], in case of mild degeneration, independent changes to these contents may occur [29]. Our data (**Figure 6**), obtained from old and moderately degenerate samples, seems to suggest greater sensitivity of T1rho to water distribution than to GAG distribution, due to a small range of water content compared to a much larger range of GAG content. This may be due to intrinsic depth-variation in water and GAG; water content varies decreases very little (~10%) from the superficial to deep layer, while GAG content increases 3-fold. Consideration of additional constituents of cartilage, as well as its structure, is needed to fully understand spatial variations of T1rho values.

There are several limitations in this study. T1rho values of structured tissues, at low spin-lock frequencies of less than 1 kHz, are susceptible to magic angle effect [34, 35 Akella, 2004, 15508163, 36], which is the variation in MR properties of fibrillar tissues with its orientation with respect to the main magnetic field (B_0) of the scanner. The patellar samples in this study, while positioned within the scanner in a consistent manner (left-to-right orientation of the sample aligned with the B_0), had sufficiently different shapes such that different parts and layers of the sample would have been subjected to the magic angle effect. In addition, our cadaveric samples were from donors of relatively advanced age, and may have altered structure (e.g., disrupted collagen network) in addition to the content. The condition of the samples also partially explains generally high values of T1rho (as high as 300 ms) found in our study. Fresh cartilage tissues from live human patients (for example harvested at the time of surgery) may be a better alternative to cadaveric specimens that degrade over time and may not

be equivalent to cartilage in vivo. Mis-registration of measurements (i.e., indentation site vs. ROI site) is also a possible source of error, but for most samples, the measurements did not seem to change abruptly at adjacent sites (e.g., **Figure 4B and C**). The deep and calcified layers of cartilage have inherently short T2 values [37] and yield little MR signal when imaged using the 2D SCMP technique. This may have resulted in inaccurate measurements of T1rho values. Techniques tailored for short T2 tissues, such as ultrashort echo time (UTE) T1rho technique [38], may provide more accurate measurements for these regions of the tissue. Lastly, indentation stiffness does not take into account the thickness of the cartilage. For the vast majority indentation sites, patellar cartilage is very thick (~5 mm) and the measured stiffness would not be affected. However for certain sites near left and right edges of the slab, relatively thin cartilage can slightly overestimate the indentation stiffness.

There are technical challenges of implementing T1rho imaging in clinical practice, despite a high potential as a mainstream protocol. There is not one T1rho sequence that is currently considered the gold standard. Many approaches exist for acquiring T1rho-weighted images and calculating T1rho values, yet these techniques do not provide the same values for the same tissue [39, 40]. Combined with this, the complexity of the human knee that contains tissues with long (synovial fluid, fat, muscle) and short (bone, ligaments, meniscus) T2 characteristics, further complicates the choice of suitable T1rho sequence. Nonetheless, T1rho is one of the most sensitive MR biomarkers of cartilage degenerate that currently available with a strong possibility of multi-vendor (i.e., General Electric, Siemens, Philips, and Canon) support. Most

currently have as a product or a research sequence at least one T1rho sequence, most popular being a 3D magnetization-prepared angle-modulated partitioned k-space spoiled gradient-echo snapshots (3D MAPSS) technique [41, 42] technique. Continued studies on the interpretation of T1rho values as it relates to the health and condition of the soft tissues of the knee, to better understand complex relationship between the MR biomarker and other tissue characteristics would be important underpinnings for an eventual clinical utility. Additionally, it is imperative clinically to establish normative values for widely used T1rho sequences, and to converge on protocols tailored for specific tissues (e.g., short vs. long T2 tissues) and conditions (e.g., early vs. late OA).

There are other MR techniques that may be sensitive to cartilage degeneration and change in GAG content. dGEMRIC [16] uses application of negatively charged intravenous contrast agent that distributes within cartilage inversely proportional to the GAG concentration. The technique is sensitive to GAG distribution [43] and, due to the use of T1 measurement, inherently resistant to magic angle artifact.[44] However, issues remain including clinical protocol such as double-dose contrast administration and exercise regimen,[16] as well as necessity for precontrast T1 measurement [45]. Sodium MRI is highly sensitive to GAG depletion [46] and applicable in vivo [47], but the necessity for specialized hardware, low signal to noise ratio (SNR) due to paucity of sodium ions, and resultant low spatial resolution are some of limitations preventing its wide use. GAG chemical exchange saturation transfer (gagCEST) [48] is yet another technique. It involves magnetization transfer [49] from protons bound to macromolecules, excited using off-resonance pulses. While promising for in vivo use [50,

51], issues including low SNR and susceptibility to main magnetic field inhomogeneity remain.

While additional work is needed to fully understand and interpret T1rho data from human articular cartilage, studies of relationship between T1rho properties, biomechanical function of cartilage and its multiple biochemical constituents, help to advance existing knowledge and provide additional guidelines. The T1rho technique, along with other techniques that are sensitive to cartilage composition, remains a viable and promising way of evaluating disease of articular cartilage non-invasively.

ACKNOWLEDGMENTS

This article was made possible in part by a grant from Veterans Affairs (I01CX000625-09A1), as well as the National Institute of Arthritis and Musculoskeletal and Skin Diseases of the National Institutes of Health (P30 AR073761). The contents of this paper are solely the responsibility of the authors and do not necessarily represent the official views of the National Institutes of Health or Veterans Affairs.

CONFLICT OF INTEREST

The authors declare that they have no conflict of interest.

REFERENCES

1. Maroudas A. Physico-chemical properties of articular cartilage. In: Freeman MAR, ed. Adult Articular Cartilage. 2nd. ed. Tunbridge Wells, England: Pitman Medical; 1979:215-290.
2. Buschmann MD, Grodzinsky AJ. A molecular model of proteoglycan-associated electrostatic forces in cartilage mechanics. J Biomech Eng. 1995; 117:179-192.
3. Andreoli TE, Bennett JC, Carpenter CCJ, Plum F, Smith LHJ. Cecil Essentials of Medicine. 3rd ed. Philadelphia, PA: W.B. Saunders Company, 1993.
4. Praemer A, Furner S, Rice DP. Musculoskeletal Conditions in the United States. Park Ridge, IL: American Academy of Orthopaedic Surgeons, 1992.
5. Schumacher HR. Primer on the Rheumatic Diseases. 10th ed. Atlanta, GA: Arthritis Foundation 1993:349.
6. Bollet AJ, Handy JR, Sturgill BC. Chondroitin sulfate concentration and protein-polysaccharide composition of articular cartilage in osteoarthritis. J Clin Invest. 1963; 42:853-859.
7. Mankin HJ, Lipiello L. Biochemical and metabolic abnormalities in articular cartilage from osteoarthritic human hips. J Bone Joint Surg Am. 1970; 52-A:424-434.
8. Squires GR, Okouneff S, Ionescu M, Poole AR. The pathobiology of focal lesion development in aging human articular cartilage and molecular matrix changes characteristic of osteoarthritis. Arthritis Rheum. 2003; 48:1261-1270.

9. Sokoloff L. Elasticity of aging cartilage. Proc Fedn Am Socs Exp Biol. 1966; 25:1089-1095.

10. Roberts S, Weightman B, Urban J, Chappell D. Mechanical and biochemical properties of human articular cartilage in osteoarthritic femoral heads and in autopsy specimens. J Bone Joint Surg Br. 1986; 68-B:278-288.

11. Kempson GE, Freeman MAR, Swanson SAV. The determination of a creep modulus for articular cartilage by indentation tests of the human femoral head. J Biomech. 1971; 4:239-250.

12. Kempson GE, Muir H, Pollard C, Tuke M. The tensile properties of the cartilage of human femoral condyles related to the content of collagen and glycosaminoglycans. Biochim Biophys Acta. 1973; 297:456-472.

13. Kempson GE. Mechanical properties of articular cartilage. In: Freeman MAR, ed. Adult Articular Cartilage. 2nd ed. Tunbridge Wells, England: Pitman Medical; 1979:333-414.

14. Chung CB, Frank LR, Resnick D. Cartilage imaging techniques: current clinical applications and state of the art imaging. Clin Orthop Relat Res. 2001(391 Suppl):S370-378.

15. Duvvuri U, Reddy R, Patel SD, Kaufman JH, Kneeland JB, Leigh JS. T1rho-relaxation in articular cartilage: effects of enzymatic degradation. Magn Reson Med. 1997; 38(6):863-867.

16. Burstein D, Velyvis J, Scott KT, Stock KW, Kim YJ, Jaramillo D, et al. Protocol issues for delayed Gd(DTPA)(2-)-enhanced MRI (dGEMRIC) for clinical evaluation of articular cartilage. Magn Reson Med. 2001; 45(1):36-41.

17. Bae WC, Temple MM, Amiel D, Coutts RD, Niederauer GG, Sah RL. Indentation testing of human cartilage: sensitivity to articular surface degeneration. Arthritis Rheum. 2003; 48(12):3382-3394.

18. Collins DH. The Pathology of Articular and Spinal Disease. London: Arnold, 1949.

19. Frank EH, Grodzinsky AJ. Cartilage electromechanics--II. A continuum model of cartilage electrokinetics and correlation with experiments. J Biomech. 1987; 20(6):629-639.

20. Han ET, Busse RF, Li X. 3D segmented elliptic-centric spoiled gradient echo imaging for the in vivo quantification of cartilage T1rho. ISMRM; 2005; Miami Beach, FL, USA; 2005. p. 473.

21. Buck FM, Bae WC, Diaz E, Du J, Statum S, Han ET, et al. Comparison of T1rho measurements in agarose phantoms and human patellar cartilage using 2D multislice spiral and 3D magnetization prepared partitioned k-space spoiled gradient-echo snapshot techniques at 3 T. AJR Am J Roentgenol. 2011; 196(2):W174-179.

22. Lyyra T, Arokoski JP, Oksala N, Vihko A, Hyttinen M, Jurvelin JS, et al. Experimental validation of arthroscopic cartilage stiffness measurement using enzymatically degraded cartilage samples. Phys Med Biol. 1999; 44(2):525-535.

23. Bae WC, Law AW, Amiel D, Sah RL. Sensitivity of indentation testing to step-off edges and interface integrity in cartilage repair. Ann Biomed Eng. 2004; 32(3):360-369.

24. Farndale RW, Sayers CA, Barrett AJ. A direct spectrophotometric microassay for sulfated glycosaminoglycans in cartilage cultures. ConnectTissue Res. 1982; 9:247-248.

25. Bae WC, Lewis CW, Levenston ME, Sah RL. Indentation testing of human articular cartilage: effects of probe tip geometry and indentation depth on intra-tissue strain. J Biomech. 2006; 39:1039-1047.

26. Wheaton AJ, Dodge GR, Elliott DM, Nicoll SB, Reddy R. Quantification of cartilage biomechanical and biochemical properties via T1rho magnetic resonance imaging. Magn Reson Med. 2005; 54(5):1087-1093.

27. Regatte RR, Akella SV, Lonner JH, Kneeland JB, Reddy R. T1rho relaxation mapping in human osteoarthritis (OA) cartilage: comparison of T1rho with T2. J Magn Reson Imaging. 2006; 23(4):547-553.

28. Zarins ZA, Bolbos RI, Pialat JB, Link TM, Li X, Souza RB, et al. Cartilage and meniscus assessment using T1rho and T2 measurements in healthy subjects and patients with osteoarthritis. Osteoarthritis Cartilage. 2010; 18(11):1408-1416.

29. Temple MM, Bae WC, Chen MQ, Lotz M, Amiel D, Coutts RD, et al. Age- and site-associated biomechanical weakening of human articular cartilage of the femoral condyle. Osteoarthritis Cartilage. 2007; 15(9):1042-1052.

30. Samosky JT, Burstein D, Eric Grimson W, Howe R, Martin S, Gray ML. Spatially-localized correlation of dGEMRIC-measured GAG distribution and mechanical stiffness in the human tibial plateau. J Orthop Res. 2005; 23(1):93-101.

31. Lyyra T, Jurvelin J, Pitkänen P, Väätäinen U, Kiviranta I. Indentation instrument for the measurement of cartilage stiffness under arthroscopic control. Med Eng Phys. 1995; 17:395-399.

32. Lyyra T, Kiviranta I, Vaatainen U, Helminen HJ, Jurvelin JS. In vivo characterization of indentation stiffness of articular cartilage in the normal human knee. J Biomed Mater Res. 1999; 48(4):482-487.

33. Maroudas A, Venn M. Chemical composition and swelling of normal and osteoarthrotic femoral head cartilage. II. Swelling. Ann Rheum Dis. 1977; 36(5):399-406.

34. Du J, Statum S, Znamirowski R, Bydder GM, Chung CB. Ultrashort TE T1rho magic angle imaging. Magn Reson Med. 2013; 69(3):682-687.

35. Wang N, Xia Y. Anisotropic analysis of multi-component T2 and T1rho relaxations in achilles tendon by NMR spectroscopy and microscopic MRI. J Magn Reson Imaging. 2013; 38(3):625-633.

36. Akella SV, Regatte RR, Wheaton AJ, Borthakur A, Reddy R. Reduction of residual dipolar interaction in cartilage by spin-lock technique. Magn Reson Med. 2004; 52(5):1103-1109.

37. Robson MD, Gatehouse PD, Bydder M, Bydder GM. Magnetic resonance: an introduction to ultrashort TE (UTE) imaging. J Comput Assist Tomogr. 2003; 27(6):825-846.

38. Du J, Carl M, Diaz E, Takahashi A, Han E, Szeverenyi NM, et al. Ultrashort TE T1rho (UTE T1rho) imaging of the Achilles tendon and meniscus. Magn Reson Med. 2010; 64(3):834-842.

39. Kim J, Mamoto K, Lartey R, Xu K, Nakamura K, Shin W, et al. Multi-vendor multi-site T(1rho) and T(2) quantification of knee cartilage. Osteoarthritis Cartilage. 2020; 28(12):1539-1550.

40. Bae WC, Malis V, Kassai Y, Miyazaki M. 3D T1rho sequences with FASE, UTE, and MAPSS acquisitions for knee evaluation. Jpn J Radiol. 2023.

41. Li X, Wyatt C, Rivoire J, Han E, Chen W, Schooler J, et al. Simultaneous acquisition of T1rho and T2 quantification in knee cartilage: repeatability and diurnal variation. J Magn Reson Imaging. 2014; 39(5):1287-1293.

42. Li X, Han ET, Busse RF, Majumdar S. In vivo T(1rho) mapping in cartilage using 3D magnetization-prepared angle-modulated partitioned k-space spoiled gradient echo snapshots (3D MAPSS). Magn Reson Med. 2008; 59(2):298-307.

43. Bashir A, Gray ML, Hartke J, Burstein D. Nondestructive imaging of human cartilage glycosaminoglycan concentration by MRI. Magn Reson Med. 1999; 41:857-865.

44. Du J, Pak BC, Znamirowski R, Statum S, Takahashi A, Chung CB, et al. Magic angle effect in magnetic resonance imaging of the Achilles tendon and enthesis. Magn Reson Imaging. 2009; 27(4):557-564.

45. Trattnig S, Burstein D, Szomolanyi P, Pinker K, Welsch GH, Mamisch TC. T1(Gd) gives comparable information as Delta T1 relaxation rate in dGEMRIC evaluation of cartilage repair tissue. Invest Radiol. 2009; 44(9):598-602.

46. Borthakur A, Shapiro EM, Beers J, Kudchodkar S, Kneeland JB, Reddy R. Sensitivity of MRI to proteoglycan depletion in cartilage: comparison of sodium and proton MRI. Osteoarthritis Cartilage. 2000; 8(4):288-293.

47. Newbould RD, Miller SR, Tielbeek JA, Toms LD, Rao AW, Gold GE, et al. Reproducibility of sodium MRI measures of articular cartilage of the knee in osteoarthritis. Osteoarthritis Cartilage. 2012; 20(1):29-35.

48. Ling W, Regatte RR, Navon G, Jerschow A. Assessment of glycosaminoglycan concentration in vivo by chemical exchange-dependent saturation transfer (gagCEST). Proc Natl Acad Sci U S A. 2008; 105(7):2266-2270.

49. Wolff SD, Balaban RS. Magnetization transfer contrast (MTC) and tissue water proton relaxation in vivo. Magn Reson Med. 1989; 10(1):135-144.

50. Schmitt B, Trattnig S, Schlemmer HP. CEST-imaging: A new contrast in MR-mammography by means of chemical exchange saturation transfer. Eur J Radiol. 2012; 81 Suppl 1:S144-146.

51. Haneder S, Apprich SR, Schmitt B, Michaely HJ, Schoenberg SO, Friedrich KM, et al. Assessment of glycosaminoglycan content in intervertebral discs using chemical exchange saturation transfer at 3.0 Tesla: preliminary results in patients with low-back pain. Eur Radiol. 2013; 23(3):861-868.

FIGURE LEGENDS

Figure 1. Sample preparation from cadaveric knees.

Figure 2. Selected T1rho-weighted images taken at spin lock times (TSL) of (**A**) 0 ms, (**B**) 20 ms, and (**C**) 80 ms, demonstrate (**D**) decreasing signal intensity with TSL at a voxel (square).

Figure 3. (**A**) Sites of indentation testing along the articular surface of patellar sample. (**B**) Regions of interest (ROI) used for determining site-specific T1rho value for comparison against the indentation data.

Figure 4. (**A**) T1rho color map of a sample demonstrating depth- and region-dependent variations. Focal areas with high T1rho values are seen (red arrows). (**B**) T1rho values at each indentation site determined using 1.2 mm diameter region of interest (ROI). (**C**) Indentation stiffness values. (**D**) Photograph of the corresponding sample showing very small superficial partial thickness cartilage defects (arrows) and ROIs from which biochemistry fragments (dashed lines) were resected. (**E**) T1rho values in ROIs representing biochemistry fragments. (**F**) Water and (**G**) sulfated glycosaminoglycan contents of the biochemistry fragments.

Figure 5. Correlation between indentation stiffness and T1rho values determined using region of interest (ROI) diamters of (**A**) 1.2, (**B**) 2.4, and (**C**) 4.8 mm.

Figure 6. Univariate regression between normalized (per sample) T1rho values and normalized contents of (**A**) water and (**B**) sulfated glycosaminoglycan per wet weight showed significant correlations. (**C**) Multivariate regression resulted in stronger correlation than either of the univariate regressions.

FIGURES

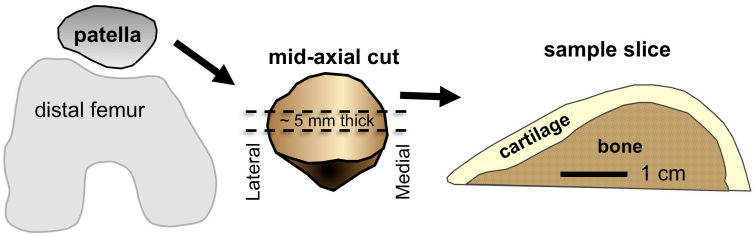

Figure 1. Sample preparation from cadaveric knees.

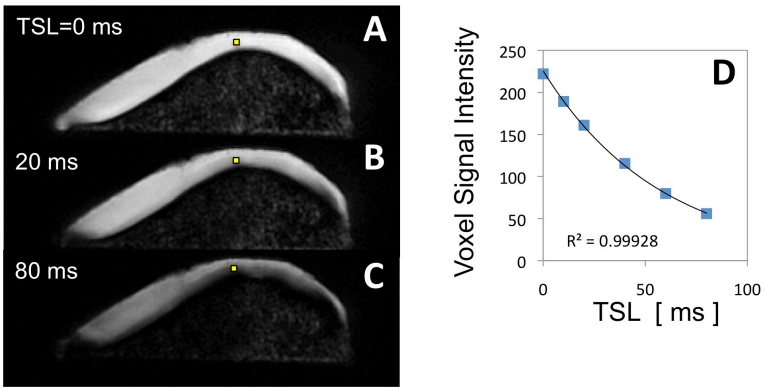

Figure 2. Selected T1rho-weighted images taken at spin lock times (TSL) of (**A**) 0 ms, (**B**) 20 ms, and (**C**) 80 ms, demonstrate (**D**) decreasing signal intensity with TSL at a voxel (square).

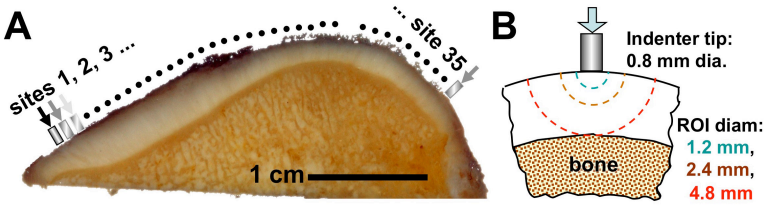

Figure 3. (**A**) Sites of indentation testing along the articular surface of patellar sample. (**B**) Regions of interest (ROI) used for determining site-specific T1rho value for comparison against the indentation data.

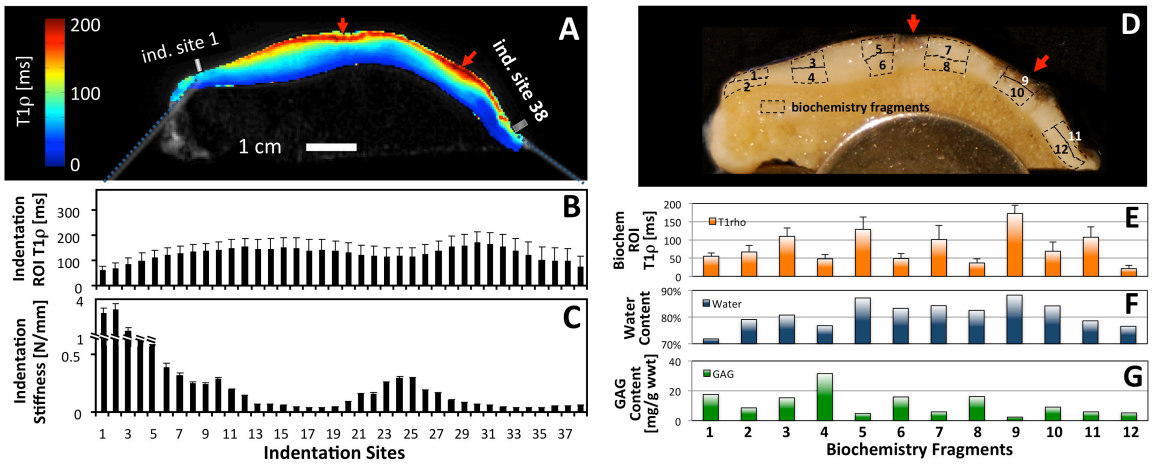

Figure 4. (**A**) T1rho color map of a sample demonstrating depth- and region-dependent variations. Focal areas with high T1rho values are seen (red arrows). (**B**) T1rho values at each indentation site determined using 1.2 mm diameter region of interest (ROI). (**C**) Indentation stiffness values. (**D**) Photograph of the corresponding sample showing very small superficial partial thickness cartilage defects (arrows) and ROIs from which biochemistry fragments (dashed lines) were resected. (**E**) T1rho values in ROIs representing biochemistry fragments. (**F**) Water and (**G**) sulfated glycosaminoglycan contents of the biochemistry fragments.

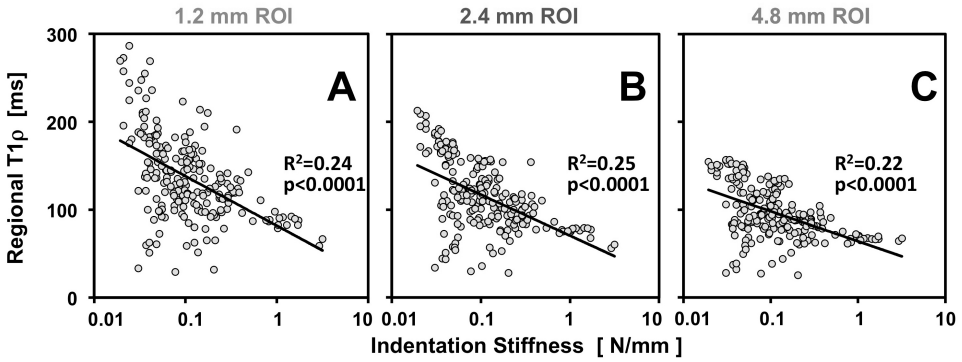

Figure 5. Correlation between indentation stiffness and T1rho values determined using region of interest (ROI) diameters of (**A**) 1.2, (**B**) 2.4, and (**C**) 4.8 mm.

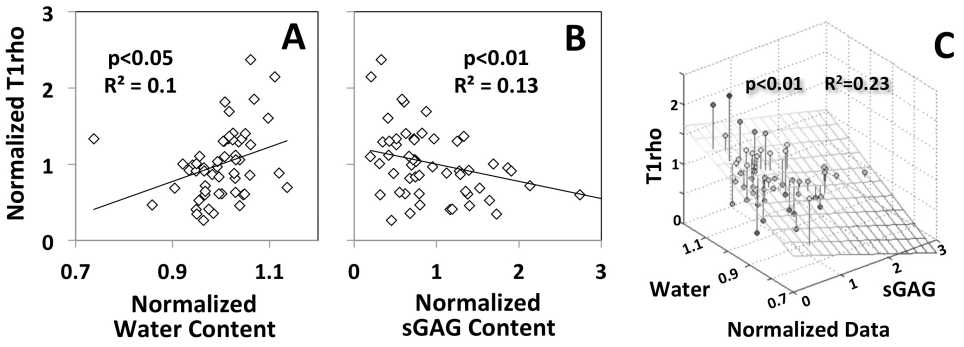

Figure 6. Univariate regression between normalized (per sample) T1rho values and normalized contents of (**A**) water and (**B**) sulfated glycosaminoglycan per wet weight showed significant correlations. (**C**) Multivariate regression resulted in stronger correlation than either of the univariate regressions.